EISSN: 2707-0425

East African Journal of Science, Technology and Innovation, Vol. 6 (Special issue 1): December 2024

Influence of rare earth doping and modifier oxides on optical and thermoluminescence properties of tellurite glasses for radiation dosimetry applications

[1]LAXMIKANTH C., [2]MAHESWARA R V*

[1]Energy and Materials Research Lab, Department of Physics, CNMS, The University of Dodoma, Tanzania
[2]Department of Chemistry, CNMS, The University of Dodoma, Tanzania

***Corresponding Author:** htnakimxal@gmail.com

Abstract

Glasses with the composition ZnF_2-MO-TeO_2:Ln_2O_3 (where M represents Zn, Cd, and Pb, and Ln represents Pr, Eu, Ho, and Er) were prepared using the melt-quench-anneal method. Absorption spectra were recorded for both undoped and rare-earth doped glasses. Judd-Ofelt (J-O) intensity parameters (Ω_2, Ω_4, and Ω_6) were determined from the spectra of the rare-earth doped glasses. The Ω_2 values were observed to be higher in ZnO-modified glasses and lower in PbO-modified glasses, indicating more asymmetric and covalent environments for Ln^{3+} ions in ZnO-modified glasses. Among the modified series, Ho^{3+} doped glasses showed lower values of Ω_4 and Ω_6, which is attributed to their significantly lower vibrational frequencies. Thermoluminescence (TL) characteristics of X-ray irradiated pure and Ln^{3+}-doped tellurite-modified glasses were studied in the temperature range of 297-473 K. Undoped glasses containing zinc, cadmium, and lead oxides exhibited single TL peaks at 423 K, 389 K, and 376 K, respectively. No additional peaks were observed upon rare-earth ion doping; however, the existing glow peak temperatures gradually shifted towards higher temperatures with an increase in the intensity of the TL light output. Among the rare-earth doped glasses, the TL light output was found to be maximum in Ho^{3+} containing any modifier. The observed TL results were discussed in light of J-O intensity parameters, showing that Ω_4 and Ω_6 are more critical than Ω_2 in optimizing the thermoluminescence properties of rare-earth-doped tellurite glasses. The trap depth parameters associated with the observed TL peaks were evaluated using Chen's formulae. These parameters suggest the potential applicability of Ho^{3+} ions doped glasses in radiation dosimetry applications.

Keywords: *Judd-Ofelt parameters; Modifier effect; Radiation dosimetry; Rare-earth ions; TeO2 glasses; Thermoluminescence*

Received: 18/06/24
Accepted: 05/12/24
Published: 20/12/24

Cite as, Laxmikanth *and* Maheswara., *(2024)*. Influence of rare earth doping and modifier oxides on optical and thermoluminescence properties of tellurite glasses for radiation dosimetry applications. *East African Journal of Science, Technology and Innovation 6 (Special issue 1).*

Introduction

The tellurium oxide (TeO_2) based glasses are materials that have attracted much interest in recent years because of their promising thermoluminescence (TL) properties in radiological dosimetry and laser technology. TeO_2 glasses are potentially valuable for applications such as very efficient gamma radiation shielding. They have versatile mechanical properties combined with a high dielectric constant; they could find applications in bandpass filters, microelectronic substrates, and solid-state battery electrolytes (ALMisned et al., 2023; Elkhoshkhany et al., 2022; Kozlovskiy et al., 2022; Mechrgui et al., 2022).

Other advantages of TeO_2-based glasses are that they are good candidates for optoelectronic, nonlinear optical fiber, and laser applications, and their stability under ionizing radiation in electronic microcircuits is also preserved (Nidzam et al., 2021). TiO_2 enhances the photocatalytic effect for water purification in tellurite glasses; their presence also affects bacterial inactivation in wastewater treatment (Isopencu et al., 2022). TeO_2 glasses have excellent properties for gamma-ray attenuation and have a high band gap energy and glass transition temperature, which is increased, so the TeO_2 glass has potential use in radiation shielding and nuclear diagnostics and monitoring activities. Besides that, highly robust optical fibers with engineered refractive index profiles could be drawn from such glasses, which find applicability in mid-infrared fiber-based photonic systems to afford more precise views of advanced scientific applications (Al-Ghamdi et al., 2022; ALMisned et al., 2022; Marzuki et al., 2022; Strutynski et al., 2022).

Fluorophosphate glass is characterized by high thermal stability and intense thermoluminescence, which makes it helpful in manufacturing robust luminescent materials (Środa et al., 2023). The ability of these glasses to dissolve higher concentrations of lithium fluoride compared to silica and borate glasses shows that they may be used in some promising technologies for high-capacity batteries (Środa et al., 2023). CdSSe-doped borosilicate glasses and Ce^{3+}-doped borosilicate glass demonstrate size-dependent and outstanding thermoluminescence intensity, respectively, indicating their use in advanced radiation detection and dosimetry (Edilashvili et al., 2023; Kaur et al., 2021).

Dy-doped glasses, especially those with 0.5 mol% Dy, show improved sensitivity, beneficial for precision dosimetry (Omar & Dhoble, 2022). Rare earth-doped glasses, including those doped with Europium and Ce^{3+}, provide high TL light output and linear response, ideal for high-resolution imaging and diagnostics (Anjaiah et al., 2019; Kaur et al., 2021). $PbCl_2$ substitution in PbO and the resulting TL emissions under UV exposure highlight potential applications in UV radiation sensors (Menezes et al., 2019). Tb^{3+}-doped Li_2O–Al_2O_3–B_2O_3 glasses and alumina-mixed borophosphate glasses, with their varying TL properties influenced by neutron reactions and γ-ray dose, are promising for neutron detection and radiation monitoring (Kalpana et al., 2017; Kawamura et al., 2021).

Despite the promising thermoluminescence (TL) properties and diverse applications of metal oxide-based glasses in radiation dosimetry, laser technologies, and optical applications, there is a lack of comprehensive understanding of how rare earth doping and the incorporation of various modifier oxides influence the optical and TL properties of these glasses. While previous studies have highlighted the beneficial effects of rare earth and other dopants in different glass matrices, the specific impacts on TeO_2-based glasses, particularly for advanced radiation detection and dosimetry, remain underexplored. This study aims to investigate the influence of rare earth (Pr^{3+}, Eu^{3+}, Ho^{3+}, and Er^{3+} with respective atomic numbers 59, 63, 67, and 68) doping and modifier oxides (ZnO, CdO, and PbO) on the optical properties, particularly aiming to correlate the Judd-Ofelt intensity parameters and thermoluminescence properties of tellurite glasses. The main objective is to determine how these modifications can enhance the performance of TeO_2 glasses in radiation dosimetry applications, thereby contributing to the development of more efficient and sensitive materials for radiation detection and other advanced optical technologies.

Materials and Methods

Glass Composition

The glasses in the current work were synthesized from high-purity raw materials including, TeO_2 (99.9% pure, Aldrich), ZnF_2 and ZnO, CdO and PbO, Pr_2O_3, Eu_2O_3, Er_2O_3, and Ho_2O_3. Different glass compositions were prepared based on various combinations of modifier oxides such as ZnO/CdO/PbO, and rare-earth dopants including Pr, Eu, Ho, and Er. The glass systems were categorized into several series:

Undoped (MT):
ZT: 40ZnF_2-10ZnO-50TeO_2,
CT: 40ZnF_2-10CdO-50TeO_2,
PT: 40ZnF_2-10PbO-50TeO_2).
Praseodymium-doped (MTPr):
ZTPr: 40ZnF_2-10ZnO-49TeO_2:1Pr_2O_3,
CTPr: 40ZnF_2-10CdO-49TeO_2:1Pr_2O_3,
PTPr: 40ZnF_2-10PbO-49TeO_2:1Pr_2O_3).

Europium-doped (MTEu):
ZTEu: 40ZnF_2-10ZnO-49TeO_2:1Eu_2O_3,
CTEu: 40ZnF_2-10CdO-49TeO_2:1Eu_2O_3,
PTEu: 40ZnF_2-10PbO-49TeO_2:1Eu_2O_3).

Holmium-doped (MTHo):
ZTHo: 40ZnF_2-10ZnO-49TeO_2:1Ho_2O_3,
CTHo: 40ZnF_2-10CdO-49TeO_2:1Ho_2O_3,
PTHo: 40ZnF_2-10PbO-49TeO_2:1Ho_2O_3).

Erbium-doped (MTEr):
ZTEr: 40ZnF_2-10ZnO-49TeO_2:1Er_2O_3,
CTEr: 40ZnF_2-10CdO-49TeO_2:1Er_2O_3,
PTEr: 40ZnF_2-10PbO-49TeO_2:1Er_2O_3).

Glass Preparation
In obtaining the desired optical and thermoluminescence properties, the glass preparation process was done through melting, quenching, and annealing. Rare-earth doped tellurite glasses, such as ZnF_2-MO-TeO_2:Ln_2O_3 glasses, were synthesized by this method. Several vital steps have to be followed in this method (Paul, 1982). Firstly, raw materials were melted. Elements such as tellurium dioxide (TeO_2), flux materials (ZnF_2), modifier oxides such as ZnO, CdO, PbO, and rare-earth oxides as Ln_2O_3 (Ln: Pr, Eu, Ho, or Er) were adopted with proper stoichiometry, mixed, and melted in a silica crucible within the temperature range of 600-700°C for half an hour to get homogeneous and good-quality glass. This ensures a homogeneous mixture and allows for the incorporation of rare-earth ions into the glass matrix. In the second step, the molten glass is rapidly cooled or quenched to prevent crystallization and to form an amorphous solid. This rapid cooling traps the disordered atomic structure, which is essential for maintaining the unique properties of the glass. Finally, the quenched glasses were then annealed at 200°C in another furnace; the step is crucial for relieving internal stresses developed during quenching and stabilizing the glass structure.

Physical Parameters
The density (d) of the glasses was determined by the standard Archimedes' principle. A direct reading balance with a readability of 0.1 mg was used for weighing. The bulk glass was suspended on a very thin copper strand that was set in the immersion liquid container; the density of the samples was determined by weighing in the liquid and air using the equation:

$$d = \frac{\text{Weight of the glass sample in air}}{\text{Weight of glass sample in pure water}} \times \text{Density of pure water} \quad (1)$$

The refractive indices (n_d) of the optically polished glasses were measured using a sodium vapor lamp (λ = 589.3 nm) on a precision Abbe's refractometer. The refractometer consists of a glass prism with a refractive index of n_o = 1.6, on whose upper surface a small specimen plate of the glass to be measured is placed. To ensure accurate measurement, the contact between the polished surface of the glass specimen and prism was kept free from air columns using mono bromonaphthalene with a refractive index of 1.658. The refractive index (n_d) of the glass specimen is then determined by illuminating it with sodium arc lamp radiation, measuring the critical angle (θ) of the light reflected into the prism, and applying the following relationship with the telescope scale calibrated to give the refractive index directly.

$$n_d = n_o \sin\theta \quad (2)$$

The density and refractive index of the glasses were used to evaluate the other physical quantities such as dopant ion concentration N_i, the polaron radius r_p, and the field strength F_i of the glasses (Elias et al., 2022).

Optical Parameters
The absorption spectra of these glasses were recorded at room temperature using a Shimadzu-3101 PC-based UV-Vis-NIR spectrophotometer, covering a wavelength range of 370-2100 nm. The analysis of radiative transitions occurring within

the $4f^n$ configuration of rare-earth ions was conducted using the Judd-Ofelt (J-O) theory. This theory involves the determination of the Judd-Ofelt parameters (Ω_λ, where λ = 2, 4, and 6). The method for determining these parameters is described in the works of cited research (Balda et al., 2007; Elias et al., 2022; Judd, 1962; Ofelt, 1962).

Judd-Ofelt Intensity Parameters (Ω_λ)

$$\Omega_\lambda = \frac{3h(2J+1)9n_d}{8\pi^2 mc\,(n_d{}^2+2)^2} T_\lambda \qquad (3)$$

Where, Planck's constant (h), ground state of the absorption transition (J), refractive index (n_d), the mass of the electron (m), speed of light in vacuum (c), and transforming parameter (T_λ) were involved in Equation 3.

Thermoluminescence and Trap Depth Parameters

X-ray Irradiation and Thermoluminescence

The synthesized glass samples were irradiated with X-rays to record the thermoluminescence light output. In this process, a Norelco X-ray tube operating at 35 kV and 10 mA is used with a monochromatic radiation wavelength of 1.541 Å. The samples were subjected to X-ray irradiation for approximately 30 minutes while kept at a constant distance of about 2 cm from the window. The irradiation was done at room temperature and in complete darkness. Thermoluminescence spectra of the X-ray-irradiated ZnF_2-MO-TeO_2 glasses were obtained in a Nucleonix-TL system by heating the sample from room temperature up to 250°C while monitoring the emitted light. It was composed of a heating device with a Kanthal alloy heating pan, a sample heating chamber made of brass, and a bakelite drawer for loading the sample; a PC-based TL analyzer, using modular electronic hardware, was used for data acquisition and analysis. The former enables controlled and reproducible heating patterns, and the latter makes sure that the sample is correctly placed in the heating chamber while temperature monitoring is maintained. The readouts of the glow curves were registered using software for acquiring, analyzing, and displaying TL data. The PMT utilized in the system is a type-9904 B from the THORN EMI Company, which assures high sensitivity and precision in measurement.

Trap Depth Parameters

Thermoluminescence peak depth trap can be determined from the peak using a variety of methods: the T_m methods (Randall et al., 1997), those involving the determination of glow curve shape (G F J Garlick & A F Gibson, 1948), and those involving both T_m and glow curve shape (Chen, 1969). The formulae by Chen (1969) are the most appropriate to analyze the TL glow curves of the glasses. The estimation of the activation energies of the glow peaks were obtained according to Chen's (1969) equations 4 and 5:

$$E_\tau = 1.52\left(\frac{k_B T_m{}^2}{\tau}\right) - 1.58(2k_B T_m) \qquad (4)$$

$$E_\delta = 0.976\left(\frac{k_B T_m{}^2}{\delta}\right) \qquad (5)$$

for first-order kinetics, where k_B is the Boltzmann constant, $\tau = (T_m - T_1)$, $\delta = (T_2 - T_m)$, and $\mu_g = \delta/(T_2 - T_1)$; Here, T_m is the glow peak temperature, and T_1 and T_2 are the temperatures at the full wave half widths of the glow peaks.

Results

Physical Parameters

Using the measured density (d, Equation 1), refractive index (n_d, Equation 2), and the calculated average molecular weight ($\bar{M}$) various physical parameters, such as lanthanide ion concentration (N_i), mean lanthanide ion separation distance (R_i), and field strength (F_i) which are crucial for understanding the certain properties of these glasses, are evaluated and presented in Table 1.

Table 1

Consolidated data on various physical properties of ZnF_2-MO-TeO_2 glasses doped with different lanthanide ions

Glass	d (gm/cm^3)	$\bar{M}$	N_i (10^{20} ions/cm^3)	R_i (Å)	F_i (10^{15} cm^{-2})	n_d
ZTPr	5.586	122.0	1.02	21.42	0.402	1.571
ZTEu	5.409	124.4	0.93	13.57	0.668	1.568
ZTHo	5.591	121.4	2.04	16.98	0.640	1.569
ZTEr	5.602	122.0	0.88	22.46	0.350	1.570
CTPr	5.608	129.0	1.02	21.39	0.403	1.574
CTEu	5.316	128.6	0.89	15.89	0.487	1.565
CTHo	5.618	128.5	2.05	16.96	0.641	1.571
CTEr	5.602	122.0	0.88	22.46	0.350	1.570
PTPr	5.663	134.7	1.03	21.35	0.405	1.576
PTEu	5.839	137.8	1.01	18.50	0.359	1.570
PTHo	5.646	133.2	2.06	16.92	0.644	1.572
PTEr	5.602	122.0	0.88	22.46	0.350	1.570

Optical Properties

Optical radiation interacts with materials in various ways depending on the material and the wavelength, resulting in optical spectra, typically observed as absorption spectra in solids. These spectra represent the variation of radiation intensity as a function of wavelength. Elements from lanthanum (Z=57) to lutetium (Z=71), known as lanthanides (Ln), are characterized by their f-block electron configuration ($4f^n\ 5s^2\ 5p^6$) in the trivalent state. As the 4f subshell fills, these ions experience a reduction in volume known as lanthanide contraction, due to imperfect shielding of the nuclear charge by the f-electrons (Jorgensen, 1962). In the present study, four rare earth ions Pr^{3+}, Eu^{3+}, Ho^{3+}, and Er^{3+} were incorporated into ZnF_2-MO-TeO_2 glasses, serving as active centres glass laser hosts due to their sharp absorption and luminescence transitions, which are weakly perturbed by surrounding ligands (Hüfner, 1978).

Absorption Spectra of Pr^{3+} Ions Doped Glasses

The absorption spectrum of Pr^{3+} doped ZnF_2-ZnO-TeO_2 glasses, recorded at room temperature in the visible and near-infrared regions, exhibited seven absorption bands (Figure 1).

Figure 1

Absorption spectrum of Pr^{3+} doped ZnF_2-ZnO-TeO_2 glass (ground state $^3H_4$

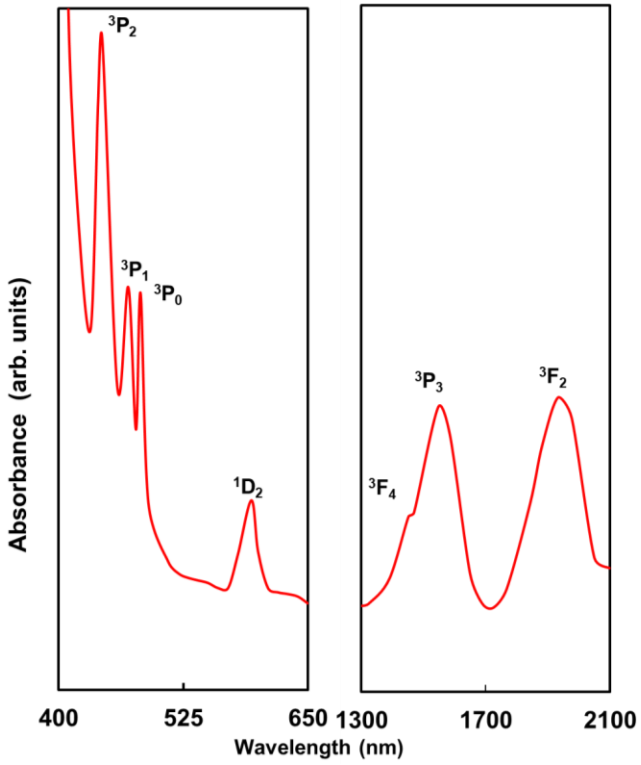

These bands correspond to the electronic transitions from $^3H_4$ to $^1D_2$, $^3P_0$, $^3P_1$, $^3P_2$, $^3F_2$, $^3F_3$, and $^3F_4$ (Carnall et al., 1968). The spectra of CTPr and PTPr glasses displayed the same bands. The spectral intensities of these bands were used in the least square fitting procedure to determine the Judd–Ofelt intensity parameters (Ω_2, Ω_4, and Ω_6) using unit tensor operators (Elias et al., 2022), as presented in Table 2.

The comparison of Judd-Ofelt parameters indicates that ZTPr glasses have the highest Ω_2 value (Table 2). For all three glasses, the Ω_λ values follow the order: $\Omega_4 > \Omega_6 > \Omega_2$. Similar trends in the Ω_λ parameter values of Pr^{3+} ions are observed in various glass matrices, with different glass hosts showing varying orders of these parameters (Babu & Jayasankar, 2001; Eyal et al., 1985; Hormadaly & Reisfeld, 1979; Quimby & Miniscalco, 1994; Yong Gyu Choi & Heo, 1997)

Table 2

Judd-Ofelt intensity parameters of ZnF_2-MO-TeO_2 glasses doped with different lanthanide ions

Glass	Ω_2 ($x10^{-20}$ cm^2)	Ω_4 ($x10^{-20}$ cm^2)	Ω_6 ($x10^{-20}$ cm^2)
ZTPr	3.78	6.33	5.78
CTPr	1.09	3.98	1.48
PTPr	1.05	3.12	1.70
ZTEu	2.87	4.85	1.02
CTEu	2.56	5.02	1.07
PTEu	2.08	1.12	4.96
ZTHo	2.73	1.25	1.03
CTHo	2.38	1.26	0.97
PTHo	2.03	1.03	0.48
ZTEr	3.14	1.19	1.43
CTEr	2.39	1.05	1.27
PTEr	1.96	0.97	1.20

Absorption Spectra of Eu^{3+} Ions Doped Glasses

The absorption spectra of Eu^{3+} doped ZnF_2-MO-TeO_2 glasses reveal sharp absorption bands corresponding to the transitions $^7F_0 \rightarrow {}^5L_6$, $^5D_2$ and $^7F_1 \rightarrow {}^5D_3$, $^5D_1$ (Carnall et al., 1968). Figure 2 illustrates the absorption spectrum of Eu^{3+} doped ZnF_2-CdO-TeO_2 glass.

Figure 2

Absorption spectrum of Eu^{3+} doped ZnF_2-CdO-TeO_2 glass

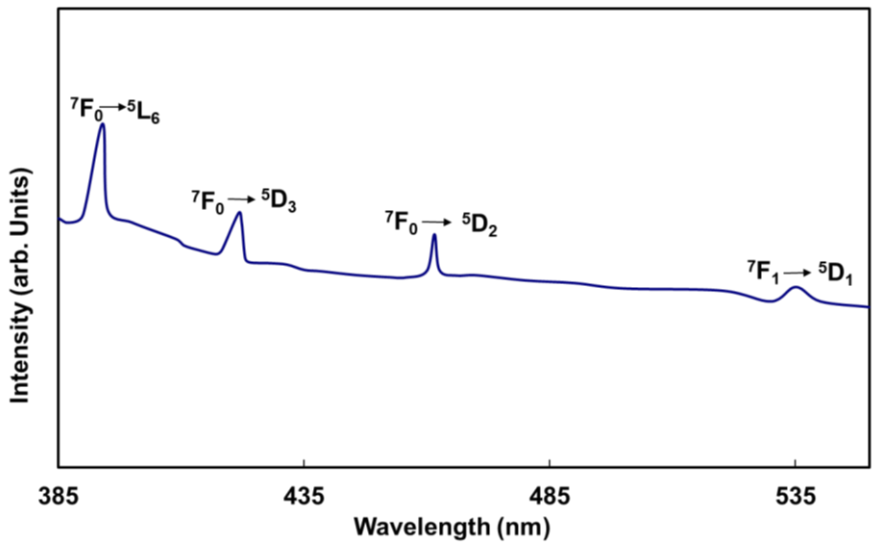

The spectra of the other two glasses exhibit bands corresponding to the same transitions. Judd–Ofelt intensity parameters (Ω_2, Ω_4, and Ω_6) for these glasses were calculated and are presented in Table 2. The J–O parameters have been observed to be following the order for ZTEu and CTEu glasses, $W_4 > W_2 > W_6$, and for the PTEu glass, $W_2 > W_4 > W_6$. The values and observed trends of the Ω_λ parameters of Eu^{3+} doped ZnF_2-MO-TeO_2 glasses are consistent with the findings of other researchers (Babu & Jayasankar, 2001; Capobianco et al., 1990, 1990; Dejneka et al., 1995; Fermi et al., 1988; Nageno et al., 1994).

Absorption Spectra of Ho^{3+} Ions Doped Glasses

The optical absorption spectra of Ho^{3+} doped ZnF_2-MO-TeO_2 glasses, recorded at room temperature over the wavelength range of 400-2100 nm, reveals eight absorption bands originating from the ground state $^5I_8$. Figure 3 presents the absorption spectrum of Ho^{3+} doped ZnF_2-PbO-TeO_2 glasses, with these levels assigned to the corresponding electronic transitions: $^5I_8 \rightarrow {}^5G_5, {}^5G_6, {}^5F_2, {}^5F_3, {}^5F_4, {}^5F_5, {}^5I_6, {}^5I_7$ (Carnall et al., 1968).

Figure 3

Absorption spectrum of Ho^{3+} doped ZnF_2-PbO-TeO_2 glass (ground state $^5I_8$)

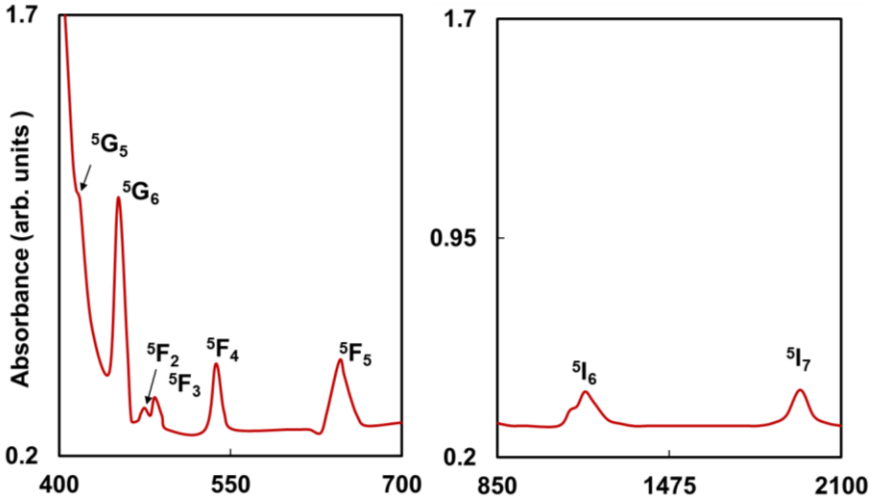

The Judd-Ofelt parameters for the three glasses are provided in Table 2. The J-O parameters have been observed to follow the trend, $W_2 > W_4 > W_6$. And are consistent with the other reported glass host systems (Hormadaly & Reisfeld, 1979; Quagliano et al., 1992; Reisfeld & Hormadaly, 1976; Tanimura et al., 1984).

Absorption Spectra of Er^{3+} Ions Doped Glasses

The optical absorption spectra of ZnF_2-MO-TeO_2 glasses doped with Er^{3+} were recorded at room temperature across the wavelength range of 370-2100 nm, exhibiting several absorption bands originating from the ground state $^4I_{15/2}$. Figure 4 shows the spectrum of the ZTEr glass).

Figure 4

Absorption spectrum of Er^{3+} doped ZnF_2-ZnO-TeO_2 glass (ground state $^4I_{15/2}$)

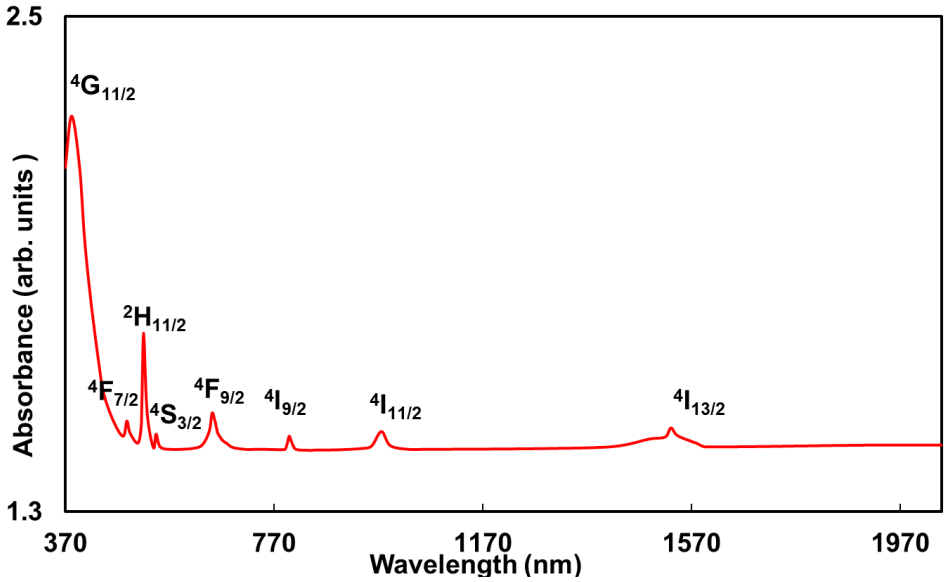

These absorption bands correspond to the following electronic transitions:

$^4I_{15/2} \rightarrow {}^4G_{11/2}, {}^4F_{7/2}, {}^2H_{11/2}, {}^4S_{3/2}, {}^4F_{9/2}, {}^4I_{9/2}, {}^4I_{11/2}, {}^4I_{13/2}$. The spectra of the other two glasses also revealed the same transitions. The Judd-Ofelt intensity parameters for these glasses were evaluated and are presented in Table 2. $W_2 > W_6 > W_4$ is the observed trend in these glasses. The comparison of the values and trends of Ω_λ observed in this study are consistent with that of other reported glass hosts (Gruen et al., 1967; Jayasankar & Kumar, 1997; Pardo et al., 2002; Takebe et al., 1994).

Summary of the Absorption Results for Ln^{3+} Doped ZnF_2-MO-TeO_2 glasses

The Judd-Ofelt intensity parameters (Ω_2, Ω_4, Ω_6) exhibit certain changes with the atomic number of rare-earth ions in different glass matrices. Figures 5, 6, and 7 illustrate the trends among Ω_2, Ω_4, and Ω_6 parameters as observed in Ln^{3+} doped ZT, CT, and PT series of glasses (Reddy et al., 2011).

Figure 5

Variation of Judd-Ofelt intensity parameters with atomic number of rare-earth ions for Ln^{3+} doped ZnF_2-ZnO-TeO_2 glasses.

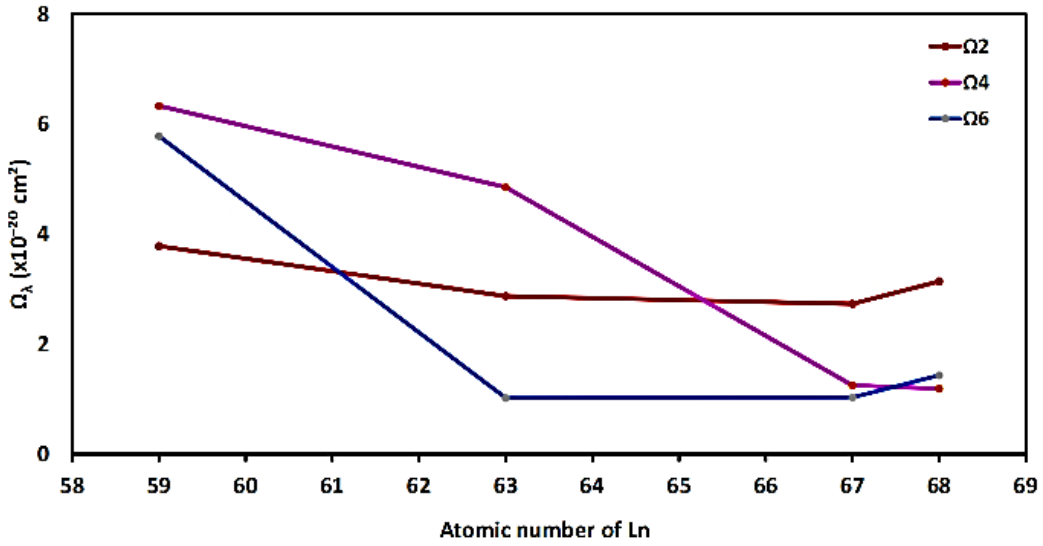

Figure 6

Variation of Judd-Ofelt intensity parameters with atomic number of rare-earth ions for Ln^{3+} doped ZnF_2-CdO-TeO_2 glasses.

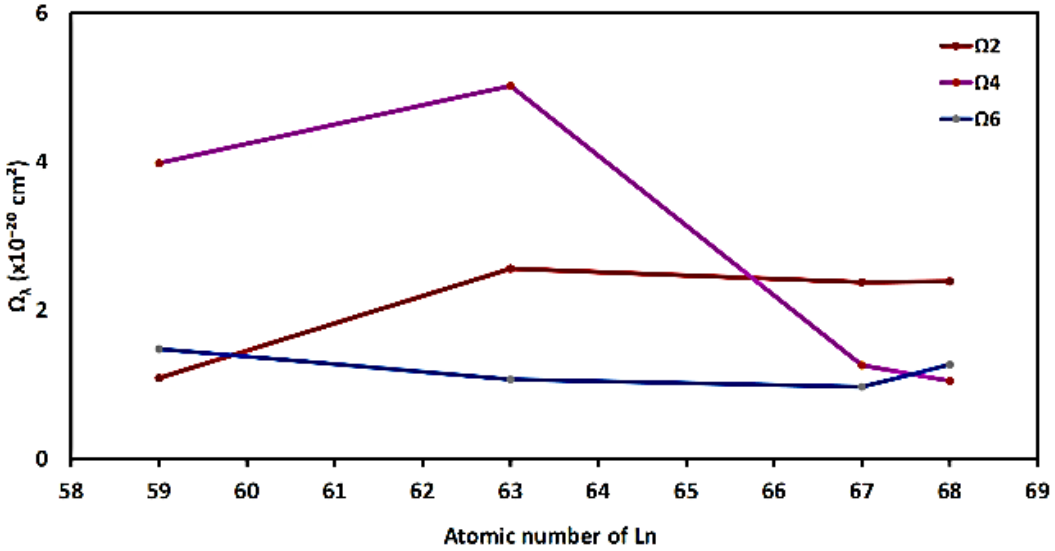

Figure 7

Variation of Judd-Ofelt intensity parameters with atomic number of rare-earth ions for Ln^{3+} doped ZnF_2-PbO-TeO_2 glasses.

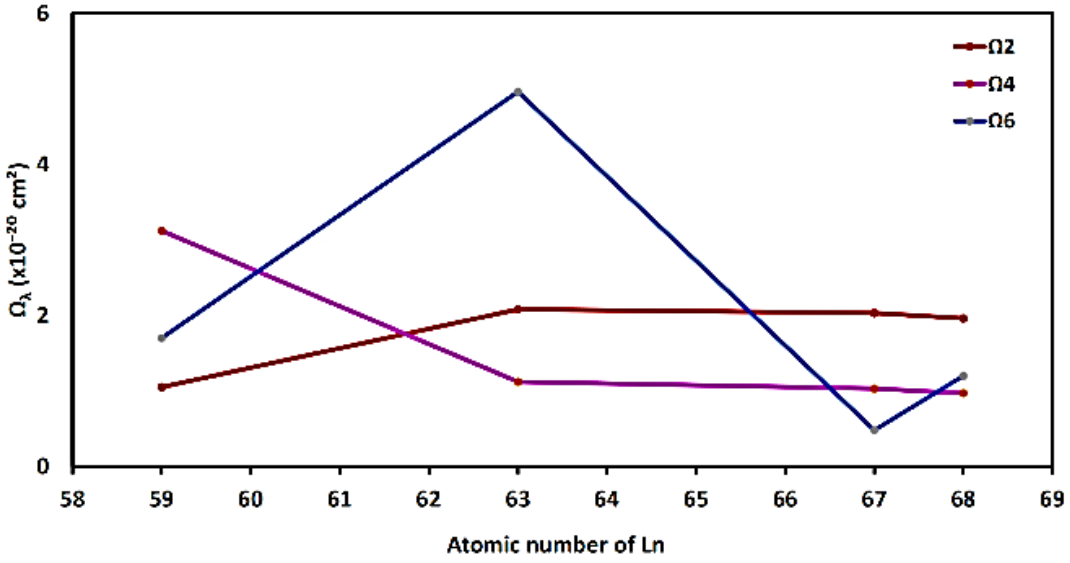

Figures 8, 9, and 10 show the variations of respective Ω_2, Ω_4, and Ω_6 parameters with atomic number of rare earths in ZT, CT, and PT series of glasses.

Figure 8

Variation of Ω_2 parameter with atomic number of rare-earth ions for Ln^{3+} doped ZnF_2-MO-TeO_2 glasses.

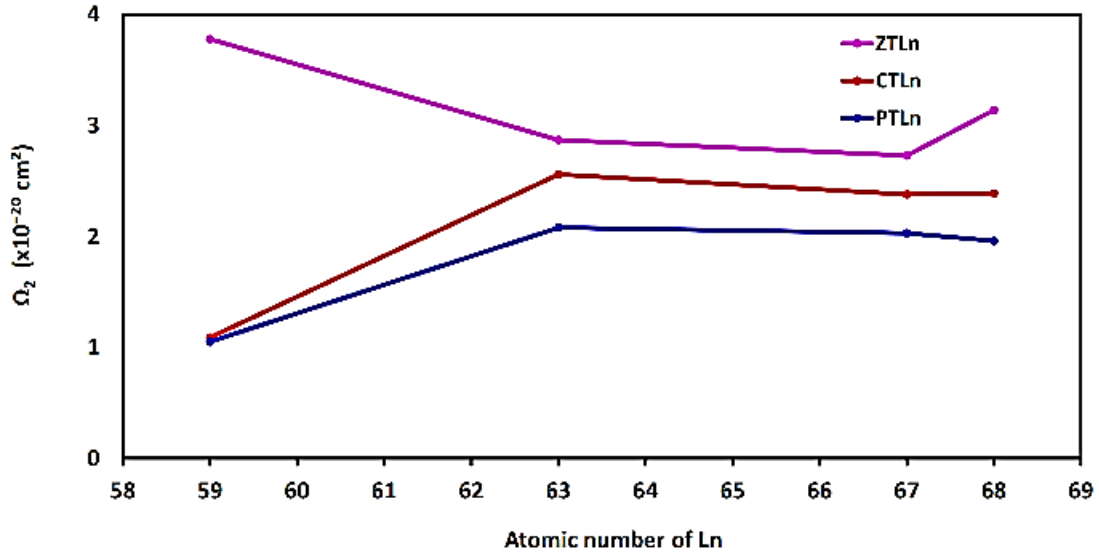

Figure 9

Variation of Ω_4 parameter with atomic number of rare-earth ions for Ln^{3+} doped ZnF_2-MO-TeO_2 glasses.

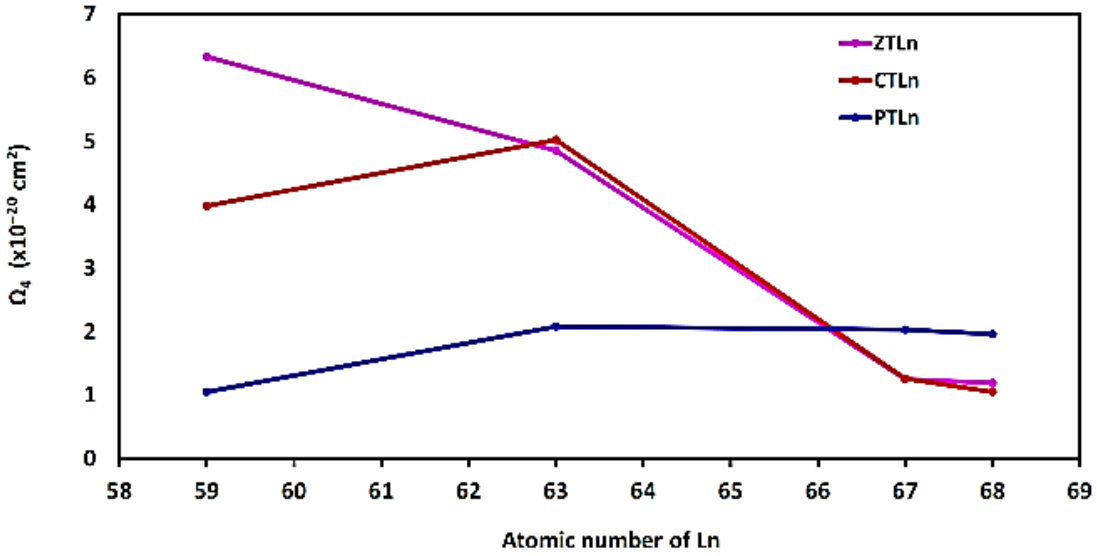

Figure 10

Variation of Ω_6 parameter with atomic number of rare-earth ions for Ln^{3+} doped ZnF_2-MO-TeO_2 glasses.

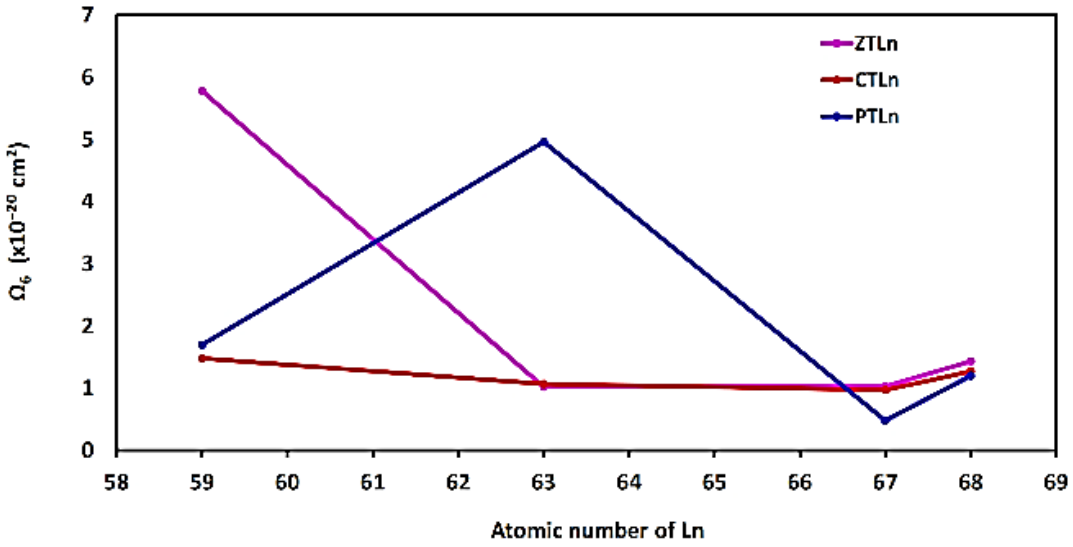

Observations show the relative higher values of Ω_2 in ZT series of glasses. Additionally, Ho^{3+}-doped glasses show relatively lower Ω_4 and Ω_6 values in ZT among the series of glasses, which could lead to deeper electron traps (Krupke, 1966). These observations centred around rare-earth ions and the modifier oxides are crucial to understand and optimize the optical properties and thermoluminescence characteristics of the glasses.

Thermoluminescence Properties

The study investigates the impact of rare earth ions on the thermoluminescence (TL) output of these glasses to evaluate their suitability for radiation dosimetry. The samples were X-ray

irradiated for half an hour to record the thermoluminescence. Figure 11 displays the TL glow curves of rare-earth free ZnF_2-MO-TeO_2 glasses recorded between 297K - 473 K.

Figure 11

Comparison plot showing TLD spectra of ZnF_2-MO-TeO_2 (pure) glasses.

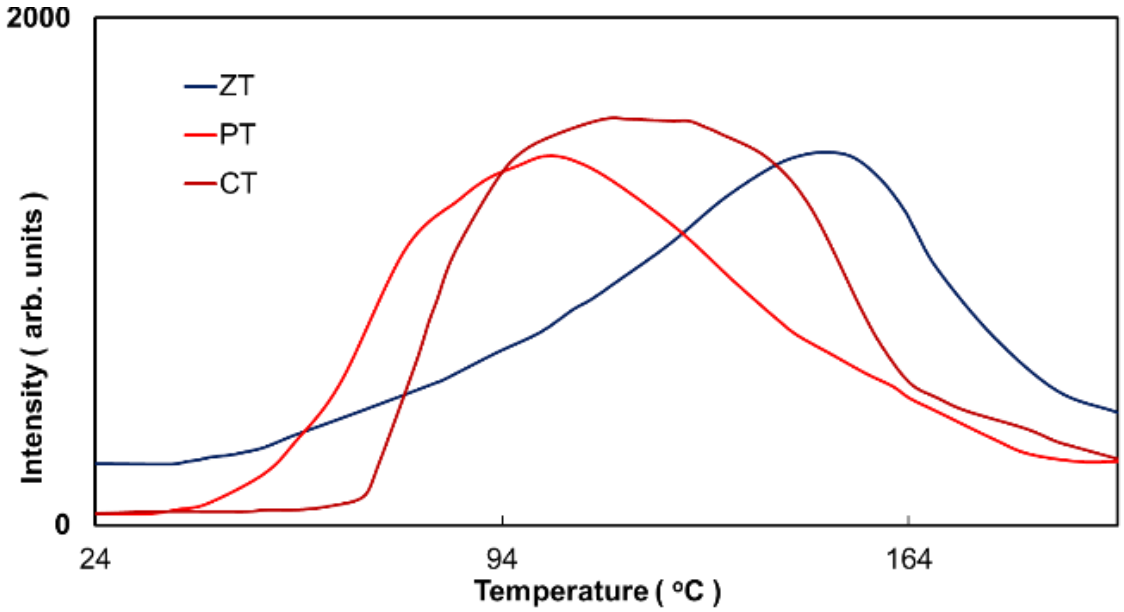

The glasses show glow peaks at 423 K, 389 K, and 376 K for ZT, CT, and PT glasses respectively. When doped with different rare earth ions, no additional peaks are observed; however, the glow peak temperatures (T_m) shift gradually to higher temperatures, with an increase in TL intensity, up to Holmium (Z=67) doped glasses. Beyond this point, as the atomic number (Z) of the doped rare-earth ion increases, the T_m shifts to lower temperatures with a decrease in glow curve intensity. Figure 12 shows the TL glow curves for Ho^{3+} doped ZnF_2-MO-TeO_2 glasses in comparison to undoped glasses.

Figure 12

Thermoluminescence emission of pure (solid line) and Ho^{3+} doped (dotted line) ZnF_2-MO-TeO_2 glasses.

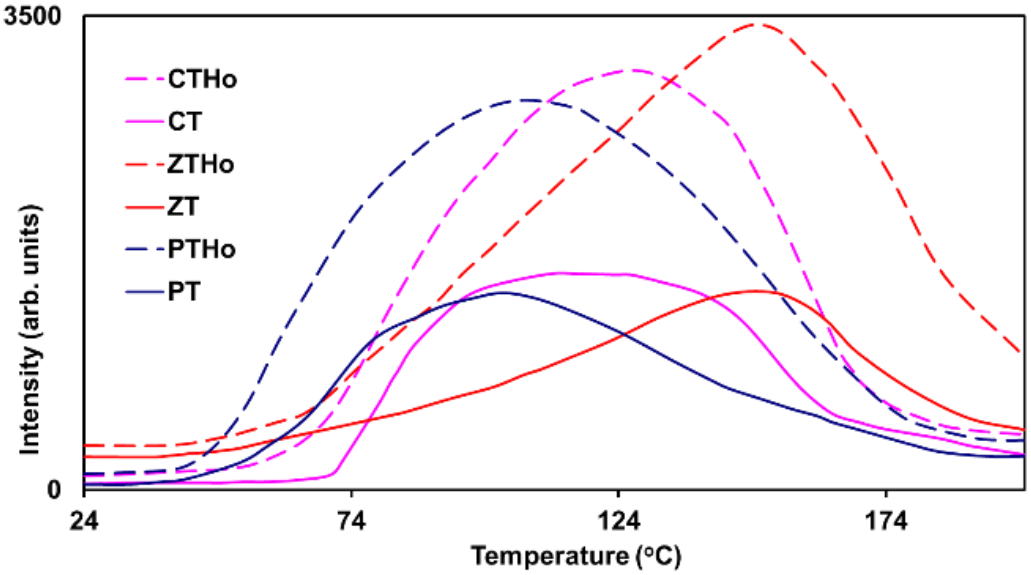

Figure 13 depicts the TL light outputs (area under the glow curves) for Ln^{3+} doped ZnF_2-MO-TeO_2 glasses.

Figure 13

Bar graph showing TL light output (area under the glow curves) of Ln^{3+} doped ZnF_2-MO-TeO_2 glasses.

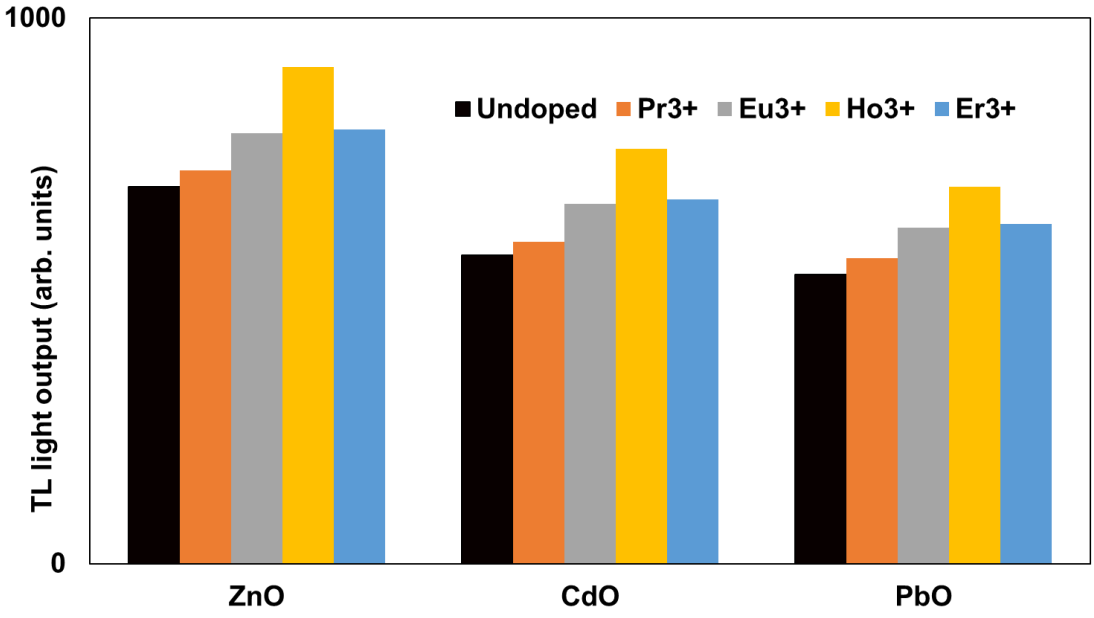

The observations indicate that Ln^{3+} doped ZT series of glasses exhibit relatively high light output compared to others. Additionally, it is evident that the Ho^{3+} doped ZnF_2-MO-TeO_2 glasses display high TL light outputs among other Ln^{3+} dopings. Over all, Ho^{3+} doped ZnF_2-ZnO-TeO_2 glass demonstrates the highest TL light output. The trap depth parameters for these glow peaks were calculated using Chen's formulae. A summary of the thermoluminescence peak positions and corresponding activation energies for the present glasses is provided in Table 3.

Table 3

Data on various trap depth parameters of ZnF_2-MO-TeO_2: Ln^{3+} glasses

Glass	T_m (K)	τ (K)	δ (K)	μ_g	E_τ (eV)	E_δ (eV)
ZT	384	35	26	0.600	0.630	0.314
ZTPr	392	35	34	0.477	0.479	0.411
ZTEu	396	40	42	0.509	0.398	0.311
ZTHo	399	27	24	0.471	0.655	0.550
ZTEr	393	35	30	0.462	0.465	0.427
CT	374	40	25	0.621	0.622	0.283
CTPr	385	40	42	0.417	0.353	0.410
CTEu	391	44	52	0.539	0.34	0.244
CTHo	396	26	19	0.422	0.673	0.685
CTEr	383	40	32	0.444	0.371	0.380
PT	417	50	28	0.641	0.690	0.289
PTPr	434	50	48	0.407	0.390	0.474
PTEu	443	36	30	0.450	0.580	0.548
PTHo	447	31	20	0.392	0.713	0.829
PTEr	426	50	41	0.451	0.355	0.367

Discussion

TeO_2 is an intermediate glass-forming oxide that does not easily form glass due to its rigid octahedral Te-O polyhedron, unlike other glass formers like GeO_2, P_2O_5, and B_2O_5. Neutron scattering experiments (Clare et al., 1989) and Raman spectral studies (Berthereau et al., 1994; S Neov et al., 1979) on TeO_2 glasses with various modifiers have shown that the fundamental building block is a trigonal bipyramid, TeO_4E, where one equatorial direction is occupied by the $5s^2$ electronic pair of tellurium with bond lengths of 1.91 Å (equatorial) and 2.08 Å (axial) (Kozhukharov et al., 1986; Sekiya et al., 1992). The Te atoms are further surrounded by longer interactions of 2.9 Å, creating a three-dimensional structure from vertex-sharing TeO_4 groups and weaker Te-O interactions (Kanth et al., 2010), forming long tetrahedral chains. Modifiers like ZnO, CdO, and PbO, when introduced, disrupt the Te-O-Te bonds, with M^{2+} ions occupying interstitial sites; however, ZnO and PbO can also form part of the glass network with ZnO_4 and

PbO_4 units. This structure is supported by IR spectral observations indicating the presence of ZnO_4 and PbO_4 units, suggesting the possibility of M-O-Te linkages (Eder et al., 2023).

Effect of Ln^{3+} Ions on Judd-Ofelt Parameters

The Ω_λ values for Ln^{3+} ions in glass systems offer information about the rare earth ions' environment in the glass lattice. The ions are randomly distributed over non-equivalent sites with varying crystal fields, as supported by simulation studies and multiple optical and ESR studies (Brodbeck & Iton, 1985; Shinn et al., 1983). Studies revealed that the ions occupying sites with non-centrosymmetric sites/ potentials significantly contribute to Ω_2 (Iftikhar, 1987; Sazali et al., 2015). These sites are associated with the asymmetry of the local environment. These sites can create an uneven distribution of the electric field around the ions, leading to changes in the electronic transitions and increasing the likelihood of certain optical phenomena. Theoretical predictions show a decreasing trend in Ω_2 values for free ions with increasing atomic number of rare-earths (Krupke, 1966). The results in this study show a similar decreasing trend up to the atomic number of Ho and then increase, differing from trends in fluoride and oxyfluoride glasses where Ω_2 increases (Oomen & van Dongen, 1989; Reisfeld, 1985). Results show a decrease of Ω_4 and Ω_6 values followed by a slow increase at higher atomic numbers, a common feature in other glass hosts and crystalline systems (Reisfeld, 1985). These values are influenced by vibrational levels associated with central rare earth ions bound to ligand atoms (Krupke, 1966). Spectral studies of vibronic transitions indicate their intensity is highest at the beginning and end of the lanthanide series (Peacock, 1975; Reisfeld, 1973, 1975).

Effect of Judd-Ofelt Parameters on TL Light Output

Ω_4 and Ω_6 values have a significant impact on the formation and stability of traps within the glass matrix. Lower values of these parameters correlate with reduced vibrational relaxation, allowing more stable and deeper traps to form. These traps can store energy more effectively, leading to higher TL output when the stored energy is released during the heating process. Higher Ω_4 and Ω_6 values would lead to shallower traps, which are less stable and release energy at lower temperatures, resulting in reduced TL intensity. While Ω_2 is sensitive to the local (short range) structural environment and covalency, its influence is more related to the immediate surroundings of the rare-earth ions rather than the long-range vibrational interactions that Ω_4 and Ω_6 are sensitive to. Based on the results and discussion, Ω_4 and Ω_6 parameters are more sensitive than Ω_2 to the overall thermoluminescence (TL) light output. The results of Ho^{3+}-doped glasses exhibit lower Ω_4 and Ω_6 values and displays highest TL light output. This empirical evidence supports the conclusion that Ω_4 and Ω_6 are more critical in determining the efficiency of TL emissions in these glasses.

Effect of Modifier Oxide on TL Light Output

Larger modifier ions (e.g., Cd^{2+} with a 1.03 Å ionic radius) increase the average distance between TeO_4 chains, leading to a weaker field around Ln^{3+} ions and lower Ω_2 compared to ZTLn (Zn^{2+} with a 0.74 Å radius). The decrease in Ω_2 for PTLn glasses is because of the increased ionic bond character of Pb^{2+} with oxygen, which results in a lower bond covalency between Ln-O bonds (Capobianco et al., 1990). This can be further favoured by the values of Ω_6, associated with host rigidity (Vermelho et al., 2003). The ZnO added into the glass introduces more of a covalent character and thus enhances stability in the network of the glass and boosts efficiency in TL light output. This can be explained by the fact that covalent bonds tend to have low vibrational frequencies, hence deeper electron traps and therefore higher TL intensity. On the other hand, the PT glasses show more of an ionic character, therefore higher vibrational frequencies. This ionic nature tends to make shallow traps, thus lowering the amount of TL light output. CT glasses exhibit intermediate behaviour between ZT and PT, which could be attributed to the reduced covalent character from ZnO.

Conclusion

This is the first systematic study on the thermoluminescence (TL) and optical properties of ZnF_2-MO-TeO_2 glasses (MO = ZnO, CdO, PbO) doped with various rare-earth ions (Pr^{3+}, Eu^{3+}, Ho^{3+}, Er^{3+}). The essential results indicate that the Judd-Ofelt intensity parameters, which include Ω_2, Ω_4, and Ω_6 are susceptible to the nature of the different rare-earth ions and modifier oxides, influencing the TL properties of the glasses. It was observed that the Ho^{3+} doped glasses amongst all the studied glasses have the highest TL output due to their lower values for Ω_4 and Ω_6, which indicated deep electron traps. Another property controlling TL output was the covalency and rigidity of the glass network, which in turn depended on the ionic radius of the modifier oxide used and its bonding nature. Ho^{3+} doped glasses demonstrated exceptional TL performance due to their unique electronic configuration and the formation of deeper electron traps. The lower values of Ω_4 and Ω_6 in these glasses favour the creation of thermally stable traps, which has the effect of increasing the intensity in TL. These make Ho^{3+} doped glasses very effective for any TL application and show their potential uses in various optical and dosimetric uses.

Recommendation

To further advance the field, it is recommended to explore additional rare-earth doped tellurite glasses to deepen the understanding of Judd-Ofelt parameters and their impact on TL properties. Investigating the long-term stability and radiation resistance of these glasses will ensure their reliability for practical applications. Additionally, developing advanced synthesis techniques to optimize doping processes and improve glass matrix homogeneity is essential for enhancing their performance and applicability in diverse fields.

Acknowledgement

We would like to express our sincere gratitude to Prof. P. Syam Prasad, Department of Physics, NIT Warangal, India, for providing the crucial research facilities.

References

Al-Ghamdi, H., Sayyed, M. I., Kumar, A., Yasmin, S., Elbashir, B. O., & Almuqrin, A. H. (2022). Effect of PbO and B2O3 on the Physical, Structural, and Radiation Shielding Properties of PbO-TeO2-MgO-Na2O-B2O3 Glasses. *Sustainability*, *14*(15), 9695. https://doi.org/10.3390/su14159695

ALMisned, G., Rabaa, E., Sen Baykal, D., Kavaz, E., Ilik, E., Kilic, G., Zakaly, H. M. H., Ene, A., & Tekin, H. O. (2023). Mechanical properties, elastic moduli, and gamma ray attenuation competencies of some TeO_2 –WO_3 –GdF_3 glasses: Tailoring WO_3 –GdF_3 substitution toward optimum behavioral state range. *Open Chemistry*, *21*(1), 20220290. https://doi.org/10.1515/chem-2022-0290

ALMisned, G., Sen Baykal, D., Susoy, G., Kilic, G., Zakaly, H. M. H., Ene, A., & Tekin, H. O. (2022). Determination of gamma-ray transmission factors of WO_3 –TeO_2 –B_2O_3 glasses using MCNPX Monte Carlo code for shielding and protection purposes. *Applied Rheology*, *32*(1), 166–177. https://doi.org/10.1515/arh-2022-0132

Anjaiah, J., Rani, G. N., Shankar, J., & Raju, P. (2019). Thermoluminescence characteristics and dosimetric aspects of Li2O-Cao-B2O3 glasses doped with rare earth ions. *AIP Conference Proceedings*, *2162*(1), 020043. https://doi.org/10.1063/1.5130253

Babu, P., & Jayasankar, C. K. (2001). Spectroscopy of Pr3+ ions in lithium borate and lithium fluoroborate glasses. *Physica B: Condensed Matter*, *301*(3), 326–340. https://doi.org/10.1016/S0921-4526(01)00239-3

Balda, R., Fernández, J., García-Revilla, S., & Fernández Navarro, J. M. (2007).

Spectroscopy and concentration quenching of the infrared emissions in Tm^3+-doped TeO_2-TiO_2-Nb_2O_5 glass. *Optics Express*, *15*(11), 6750. https://doi.org/10.1364/OE.15.006750

Berthereau, A., Le Luyer, Y., Olazcuaga, R., Le Flem, G., Couzi, M., Canioni, L., Segonds, P., Sarger, L., & Ducasse, A. (1994). Nonlinear optical properties of some tellurium (IV) oxide glasses. *Materials Research Bulletin*, *29*(9), 933–941. https://doi.org/10.1016/0025-5408(94)90053-1

Brodbeck, C. M., & Iton, L. E. (1985). The EPR spectra of Gd3+ and Eu2+ in glassy systems. *The Journal of Chemical Physics*, *83*(9), 4285–4299. https://doi.org/10.1063/1.449041

Capobianco, J. A., Proulx, P. P., Bettinelli, M., & Negrisolo, F. (1990). Absorption and emission spectroscopy of ${\mathrm{Eu}}^{3+}$ in metaphosphate glasses. *Physical Review B*, *42*(10), 5936–5944. https://doi.org/10.1103/PhysRevB.42.5936

Carnall, W. T., Fields, P. R., & Rajnak, K. (1968). Electronic Energy Levels of the Trivalent Lanthanide Aquo Ions. III. Tb3. *Journal of Chemical Physics*, *49*, 4447–4449.

Chen, R. (1969). On the Calculation of Activation Energies and Frequency Factors from Glow Curves. *Journal of Applied Physics*, *40*(2), 570–585. https://doi.org/10.1063/1.1657437

Clare, A. G., Wright, A. C., Sinclair, R. N., Galeener, F. L., & Geissberger, A. E. (1989). A neutron diffraction investigation of the structure of vitreous As2O3. *Journal of Non-Crystalline Solids*, *111*(2), 123–138. https://doi.org/10.1016/0022-3093(89)90274-3

Dejneka, M., Snitzer, E., & Riman, R. E. (1995). Blue, green and red fluorescence and energy transfer of Eu3+ in fluoride glasses. *Journal of Luminescence*, *65*(5), 227–245. https://doi.org/10.1016/0022-2313(95)00073-9

Eder, F., Weil, M., Pramanik, P., & Mathieu, R. (2023). The Cobalt(II) Oxidotellurate(IV) Hydroxides Co2(TeO3)(OH)2 and Co15(TeO3)14(OH)2. *Crystals*, *13*(2), 176. https://doi.org/10.3390/cryst13020176

Elias, A. M., Mwanga, S. F., Mwankemwa, B., J, A., & C, L. (2022). Influence of Bi+ ions on photoluminescence properties of Tm2O3 doped borotellurite glasses for the near-infrared emission applications. *Optical Materials*, *125*, 112140. https://doi.org/10.1016/j.optmat.2022.112140

Elkhoshkhany, N., Marzouk, S., El-Sherbiny, M., Ibrahim, H., Burtan-Gwizdala, B., Alqahtani, M. S., Hussien, K. I., Reben, M., & Yousef, E. S. (2022). Investigation of Structural, Physical, and Attenuation Parameters of Glass: TeO2-Bi2O3-B2O3-TiO2-RE2O3 (RE: La, Ce, Sm, Er, and Yb), and Applications Thereof. *Materials*, *15*(15), 5393. https://doi.org/10.3390/ma15155393

Eyal, M., Greenberg, E., Reisfeld, R., & Spector, N. (1985). Spectroscopy of praseodymium(III) in zirconium fluoride glass. *Chemical Physics Letters*, *117*(2), 108–114. https://doi.org/10.1016/0009-2614(85)85216-7

Fermi, F., Tellini, L., Ingletto, G., Vinattieri, A., & Bettinelli, M. (1988). Absorption and luminescence spectroscopy of Eu3+ in lead silicate glasses. *Inorganica Chimica Acta*, *150*(1), 141–146. https://doi.org/10.1016/S0020-1693(00)87635-5

G F J Garlick & A F Gibson. (1948). The Electron Trap Mechanism of Luminescence in Sulphide and Silicate Phosphors. *Proceedings of the Physical Society*, *60*(6), 574. https://doi.org/10.1088/0959-5309/60/6/308

Gruen, D. M., Dekock, C. W., & Mcbeth, R. L. (1967). Electronic Spectra of Lanthanide Compounds in the Vapor Phase. In *Lanthanide/Actinide Chemistry* (Vol. 71, pp. 102–121). *American Chemical Society*. https://doi.org/10.1021/ba-1967-0071.ch008

Hormadaly, J., & Reisfeld, R. (1979). Intensity parameters and laser analysis of Pr3+ and Dy3+ in oxide glasses. *Journal of Non-Crystalline Solids*, *30*(3), 337–348.

https://doi.org/10.1016/0022-3093(79)90171-6
Hüfner, S. (1978). *Optical spectra of transparent rare earth compounds*. Academic Press.
Iftikhar, K. (1987). Hypersensitivity in the 4f–4f absorption spectra of lanthanide(III) complexes. *Inorganica Chimica Acta*, *129*(2), 261–264. https://doi.org/10.1016/S0020-1693(00)86672-4
Edilashvili, V., Blagidze, Yu., Gogolin, O., Tsitsishvili, E. (2023). Thermoluminescence peculiarities of $CdS_{1-x}Se_x$–doped borosilicate glasses. *Chalcogenide Letters*, *20*(4), 235–241. https://doi.org/10.15251/CL.2023.204.235
Isopencu, G., Eftimie, M., Melinescu, A., Dancila, A. M., & Mares, M. (2022). Recycling of Glass Waste by Deposition of TiO2 for the Intensification of the Photocatalytic Effect in the Purification of Wastewater. *Coatings*, *12*(11), 1794. https://doi.org/10.3390/coatings12111794
Jayasankar, C. K., & Kumar, V. V. R. K. (1997). Spectroscopic properties of Er3+ ions in cadmium and alkali cadmium borosulphate glasses. *Pramana*, *48*(6), 1151–1160. https://doi.org/10.1007/BF02845890
Jorgensen, C. K. (1962). *Absorption spectra and chemical bonding in complexes*.
Judd, B. R. (1962). Optical Absorption Intensities of Rare-Earth Ions. *Physical Review*, *127*(3), 750–761. https://doi.org/10.1103/PhysRev.127.750
Kalpana, T., Sanyal, B., Gandhi, Y., Ravi Kumar, V., Baskaran, G. S., Bragiel, P., Piasecki, M., & Veeraiah, N. (2017). Thermoluminescence features of alumina-mixed borophosphate glasses with Tb3+ ions for dosimetric applications. *International Journal of Applied Glass Science*, *8*(2), 188–195. https://doi.org/10.1111/ijag.12223
Kanth, C. L., Reddy, Y. R., Babu, K. R., & Anjaiah, J. (2010). *Study on Certain Physical Properties of ZnF2-CdO-TeO2:Cr2O3 Glasses*.
Kaur, R., Rakesh, R. B., Mhatre, S. G., Bhatia, V., Kumar, D., Singh, H., Singh, S. P., & Kumar, A. (2021). Thermoluminescence, structural and optical properties of Ce3+ doped borosilicate doped glasses. *Journal of Materials Science: Materials in Electronics*, *32*(13), 18381–18396. https://doi.org/10.1007/s10854-021-06382-8
Kawamura, I., Kawamoto, H., Fujimoto, Y., Koshimizu, M., Okada, G., Wakabayashi, G., Nogami, M., Hitomi, K., Watanabe, K., Yanagida, T., & Asai, K. (2021). Neutron detection via thermoluminescence of Tb3+-doped Li2O–Al2O3–B2O3 glasses. *Japanese Journal of Applied Physics*, *60*(3), 036002. https://doi.org/10.35848/1347-4065/abdf7d
Kozhukharov, V., Bürger, H., Neov, S., & Sidzhimov, B. (1986). Atomic arrangement of a zinc-tellurite glass. *Polyhedron*, *5*(3), 771–777. https://doi.org/10.1016/S0277-5387(00)84436-8
Kozlovskiy, A., Shlimas, D. I., Zdorovets, M. V., Popova, E., Elsts, E., & Popov, A. I. (2022). Investigation of the Efficiency of Shielding Gamma and Electron Radiation Using Glasses Based on TeO2-WO3-Bi2O3-MoO3-SiO to Protect Electronic Circuits from the Negative Effects of Ionizing Radiation. *Materials*, *15*(17), 6071. https://doi.org/10.3390/ma15176071
Krupke, W. F. (1966). Optical Absorption and Fluorescence Intensities in Several Rare-Earth-Doped \mathrmY_2\mathrmO_3 and La\mathrmF_3 Single Crystals. *Phys. Rev.*, *145*(1), 325–337. https://doi.org/10.1103/PhysRev.145.325
Marzuki, A., Ega, F. D., & Saraswati, A. (2022). Effect of B2O3 addition on thermal and optical properties of TeO2–ZnO–Bi2O3–TiO2 glasses. *Materials Research Express*, *9*(2), 025203–025203. https://doi.org/10.1088/2053-1591/ac55c5
Mechrgui, I., Ben Gouider Trabelsi, A., Alkallas, Fatemah. H., Nasri, S., & Elhouichet, H. (2022). Mixed Ionic and Electronic

Conduction in TeO2-ZnO-V2O5 Glasses towards Good Dielectric Features. *Materials*, *15*(21), 7659. https://doi.org/10.3390/ma15217659

Menezes, D. L. A., Bannwart, E. S., De Souza, J. E., & Rojas, S. S. (2019). Thermoluminescence emission on lead oxychloroborate glasses under UV exposure. *Luminescence*, *34*(8), 918–923. https://doi.org/10.1002/bio.3691

Nageno, Y., Takebe, H., Morinaga, K., & Izumitani, T. (1994). Effect of modifier ions on fluorescence and absorption of Eu3+ in alkali and alkaline earth silicate glasses. *Journal of Non-Crystalline Solids*, *169*(3), 288–294. https://doi.org/10.1016/0022-3093(94)90324-7

Nidzam, N. N. S., Umar, S. A., Halimah, M. K., Marian, M. M., Najwa, Z. W., Jufa, M. S., Syahirah, M. T., Zuhasanah, Z., Azlan, M. N., Geidam, I. G., & Boukhris, I. (2021). *Dielectric Constant, Metallization Criterion and Optical Properties of CuO Doped TeO2-B2O3 Glasses*. https://doi.org/10.21203/rs.3.rs-1175617/v1

Ofelt, G. S. (1962). Intensities of Crystal Spectra of Rare-Earth Ions. *Journal of Chemical Physics*, *37*, 511–520.

Omar, R. S., & Dhoble, S. J. (2022). Chapter 14—Dosimetric properties of gamma-irradiated borate materials. In S. Dhoble, V. Chopra, V. Nayar, G. Kitis, D. Poelman, & H. Swart (Eds.), *Radiation Dosimetry Phosphors* (pp. 355–403). Woodhead Publishing. https://doi.org/10.1016/B978-0-323-85471-9.00009-9

Oomen, E. W. J. L., & van Dongen, A. M. A. (1989). Europium (III) in oxide glasses: Dependence of the emission spectrum upon glass composition. *Journal of Non-Crystalline Solids*, *111*(2), 205–213. https://doi.org/10.1016/0022-3093(89)90282-2

Pardo, J. A., Peña, J. I., Merino, R. I., Cases, R., Larrea, A., & Orera, V. M. (2002). Spectroscopic properties of Er3+ and Nd3+ doped glasses with the 0.8CaSiO3–0.2Ca3(PO4)2 eutectic composition. *Journal of Non-Crystalline Solids*, *298*(1), 23–31. https://doi.org/10.1016/S0022-3093(01)01043-2

Paul, A. (1982). *Chemistry of Glasses*. Springer Netherlands. https://doi.org/10.1007/978-94-009-5918-7

Peacock, R. D. (1975). The intensities of lanthanide f ↔ f transitions. In E. Nieboer, C. K. Jørgensen, R. D. Peacock, & R. Reisfeld (Eds.), *Rare Earths* (pp. 83–122). Springer Berlin Heidelberg.

Quagliano, J. R., Richardson, F. S., & Reid, M. F. (1992). Comparative analyses of Nd3+ (4f3) energy level structures in various crystalline hosts. *Journal of Alloys and Compounds*, *180*(1), 131–139. https://doi.org/10.1016/0925-8388(92)90372-G

Quimby, R. S., & Miniscalco, W. J. (1994). Modified Judd–Ofelt technique and application to optical transitions in Pr3+-doped glass. *Journal of Applied Physics*, *75*(1), 613–615. https://doi.org/10.1063/1.355794

Randall, J. T., Wilkins, M. H. F., & Oliphant, M. L. E. (1997). Phosphorescence and electron traps—I. The study of trap distributions. *Proceedings of the Royal Society of London. Series A. Mathematical and Physical Sciences*, *184*(999), 365–389. https://doi.org/10.1098/rspa.1945.0024

Reddy, C. M., Mallikarjuna, K., Reddy, B. S., Raju, K. V., Deva, B., & Raju, P. (2011). *Optical absorption and photoluminescence studies of Dy 3+: LCZSFB glasses*. https://api.semanticscholar.org/CorpusID:56403533

Reisfeld, R. (1973). Spectra and energy transfer of rare earths in inorganic glasses. *Rare Earths*, 53–98.

Reisfeld, R. (1975). Radiative and non-radiative transitions of rare-earth ions in glasses. In E. Nieboer, C. K. Jørgensen, R. D. Peacock, & R. Reisfeld (Eds.), *Rare Earths* (pp. 123–175). Springer Berlin Heidelberg.

Reisfeld, R. (1985). Luminescence and prediction of transition probabilities for solar energy and lasers. *Proceedings of the International Rare Earth Conference*, *112*(1), 9–18.

https://doi.org/10.1016/0022-5088(85)90003-7

Reisfeld, R., & Hormadaly, J. (1976). Optical intensities of holmium in tellurite, calibo, and phosphate glasses. *The Journal of Chemical Physics*, *64*(8), 3207–3212. https://doi.org/10.1063/1.432659

S Neov, V Kozhukharov, I Gerasimova, K Krezhov, & B Sidzhimov. (1979). A model for structural recombination in tellurite glasses. *Journal of Physics C: Solid State Physics*, *12*(13), 2475. https://doi.org/10.1088/0022-3719/12/13/012

Sazali, E. S., Sahar, Md. R., & Rohani, Md. S. (2015). Optical Investigation of Erbium Doped Lead Tellurite Glass: Judd-Ofelt Analysis. *International Conference on Solid State Physics 2013 (ICSSP'13)*, *2*(10, Part B), 5241–5245. https://doi.org/10.1016/j.matpr.2015.11.029

Sekiya, T., Mochida, N., Ohtsuka, A., & Tonokawa, M. (1992). Raman spectra of MO1/2TeO2 (M = Li, Na, K, Rb, Cs and Tl) glasses. *Journal of Non-Crystalline Solids*, *144*, 128–144. https://doi.org/10.1016/S0022-3093(05)80393-X

Shinn, M. D., Sibley, W. A., Drexhage, M. G., & Brown, R. N. (1983). Optical transitions of ${\mathrm{Er}}^{3+}$ ions in fluorozirconate glass. *Physical Review B*, *27*(11), 6635–6648. https://doi.org/10.1103/PhysRevB.27.6635

Środa, M., Świontek, S., & Olejniczak, Z. (2023). Thermal and thermoluminescence properties of LiF-BaO-P2O5 glass. *Journal of Non-Crystalline Solids*, *599*, 121983. https://doi.org/10.1016/j.jnoncrysol.2022.121983

Strutynski, C., Evrard, M., Gendre, A. L., Maldonado, A., Désévédavy, F., Gadret, G., Jules, J., & Smektala, F. (2022). Physicochemical Properties and Fiber-Drawing Ability of Tellurite Glasses in the TeO2-ZnO-Y2O3 Ternary System. *Materials*, *15*(3), 1177–1177. https://doi.org/10.3390/ma15031177

Takebe, H., Nageno, Y., & Morinaga, K. (1994). Effect of Network Modifier on Spontaneous Emission Probabilities of Er3+ in Oxide Glasses. *Journal of the American Ceramic Society*, *77*(8), 2132–2136. https://doi.org/10.1111/j.1151-2916.1994.tb07108.x

Tanimura, K., Shinn, M. D., Sibley, W. A., Drexhage, M. G., & Brown, R. N. (1984). Optical transitions of \mathrmHo^3+ ions in fluorozirconate glass. *Phys. Rev. B*, *30*(5), 2429–2437. https://doi.org/10.1103/PhysRevB.30.2429

Vermelho, M. V. D., Gouveia-Neto, A. S., Amorim, H. T., Cassanjes, F. C., Ribeiro, S. J. L., & Messaddeq, Y. (2003). Temperature investigation of infrared-to-visible frequency upconversion in erbium-doped tellurite glasses excited at 1540nm. *Proceedings of the 2002 International Conference on Luminescence and Optical Spectroscopy of Condensed Matter*, *102–103*, 755–761. https://doi.org/10.1016/S0022-2313(02)00637-3

Yong Gyu Choi, & Heo, J. (1997). 1.3 μm emission and multiphonon relaxation phenomena in PbO□Bi2O3□Ga2O3 glasses doped with rare-earths. *Journal of Non-Crystalline Solids*, *217*(2), 199–207. https://doi.org/10.1016/S0022-3093(97)00189-0